

# Improvement of the performance of thin-film CdS/PbS solar cells using low-cost ZnO-based alloys as front electrode

H. A. MOHAMED<sup>a,b</sup>, M. R. AHMED<sup>a</sup>

<sup>a</sup>Department of Physics, Faculty of Science, Sohag University, 82524 Sohag, Egypt

<sup>b</sup>Department of Physics, College of Sciences, King Saud University, 11451 Riyadh, KSA.

All thin film solar cells require the use of transparent conductive electrodes such as indium tin oxide (ITO) due to its unique combination of transparency, high conductivity, durability, and favourable surface properties. Indium, however, is a rare and expensive metal; proposed large-area installations of photovoltaic (PV) cells will add further strain to global indium supply. Transparent conductive materials that are abundant, inexpensive, and enable efficient thin film solar cells must therefore be developed. Zinc oxide (ZnO), tin doped zinc oxide (ZnO:Sn), aluminum doped zinc (ZnO:Al) and indium doped zinc oxide (ZnO:In) were theoretically investigated as alternatives transparent conductive oxides (TCO) to indium tin oxide that used as front electrode in CdS/PbS thin-film solar cells. The effect of optical and recombination losses as well as the reflectivity from metallic back contact were investigated in this work. It was found that the spectral quantum efficiency depends on the width of space-charge region ( $W$ ) and the thickness of absorber layer ( $d_{\text{PbS}}$ ). The maximum short-circuit current density of about 20.9 mA/cm<sup>2</sup> was achieved at  $W= 3\mu\text{m}$  and  $d_{\text{PbS}}=2\mu\text{m}$  for ZnO:Al. The average optical losses due to reflection from all interfaces and due to absorption in CdS and TCO layers were about 32%. The total reflected back contact lead to increase the short-circuit current density by 20% and hence the efficiency of CdS/PbS cell recorded a value of 7.89 % for ZnO:Al.

(Received November 20, 2015; accepted June 7, 2017)

**Keywords:** CdS-PbS solar cell, low cost transparent electrodes, optical losses, recombination losses

## 1. Introduction

Thin film solar cells based on lead sulfide (PbS) as an active absorbing layer in a solar cell can be considered unusual as the expected efficiency would be lower than what is actually attained in more conventional CdTe/CdS or CIGS/CdS solar cells. The recent advancements in this types of solar cells [1-5] have shown the convenience of developing solar cells based on PbS. PbS is a narrow gap semiconductor, which differs from the majority of semiconductors in the character of temperature and deformational dependence of its band gap; it is also known that the latter in PbS is very sensitive to the grain size (much more than in classic semiconductors like Si), which make it a good candidate for nanostructured devices. Besides, the effect of multiple exciton generation was recently discovered in nanostructures of PbS and similar semiconductor PbSe [6], which is very promising for solar cell applications.

At the present stage of development of industry and technology of photovoltaic solar cell devices, the most important problem is the production cost, which includes the cost of materials and that of technologies involved as well as the energy consumption in technological processes. Recently, several theoretical attempts have been carried out to study and improve the efficiency of thin film CdS/PbS heterojunction solar cells [7, 8].

This type of solar cells is composed of four layers: 1) the front electrode that is made from transparent conducting oxide (TCO), 2) window layer that is made from CdS, 3) absorber layer that is made from PbS and 4) metallic back contact layer that is made from Al or Au. Each layer of them must satisfy some physical properties. For example; the transparent conducting oxides (TCO) layer must have transmission more than 85% in visible region and sheet resistance less than 10  $\Omega$ /square at room temperature as well as good adhesion to glass substrate [9, 10].

Thin film photovoltaic (PV) solar cells such as CdS/CdTe and CdS/PbS require the use of transparent conductive electrodes. Indium oxide (ITO) is currently the transparent conductor choice for these applications, due to its unique combination of transparency, high conductivity, durability, and favourable surface properties. Indium, however, is a rare and expensive metal; proposed large-area installations of PV cells will add further strain to global indium supply. Transparent conductive materials that are abundant, inexpensive, and enable efficient thin film solar cells must therefore be developed. ZnO has been actively investigated as an alternative material to ITO because ZnO is non-toxic, inexpensive and abundant material. It is also chemically stable so it is used for the production of solar cells [11- 13].

The main objective of this paper is to assess the effects of ZnO and its alloys such as ZnO:Sn, ZnO:Al and

ZnO:In as front electrode on the calculation of CdS/PbS solar cell parameters. The optical losses due to reflection from difference interfaces and absorption in both TCO and CdS layers will be considered. Moreover, the recombination losses at front and back surface of PbS layer will be studied in this work. Finally, the effect of reflectivity of metallic back contact on the cell parameters will be taken into consideration.

## 2. Theoretical concepts

### 2.1. Reflection and absorption losses

The normal incident light will penetrate glass, TCO, CdS layers before reaching the active PbS absorber layer. Through this path, a part of the incident light will be lost in these layers due to reflection from air-glass, glass-TCO, TCO-CdS and CdS-PbS interfaces and absorption in glass, TCO and CdS layers.

There are two methods to calculate the transmitted light that will reach the absorber layer:

#### 2.1.1. Method one

In this method, the reflection may occur due to a certain part of the incident light will reflect at the interface between any two layer. According to the Fresnel equations, the reflection coefficient (reflectivity) from the interface between two contacting materials is determined by their refractive indices  $n_1$  and  $n_2$ :

$$R_f = \frac{(n_1 - n_2)^2}{(n_1 + n_2)^2} \quad (1)$$

In the case of electrically conductive materials, the refractive index contains an imaginary part and is written as  $n^* = n - ik$ , where  $n$  is the refractive index, and  $k$  is the extinction coefficient. The reflection coefficient from the interface is defined as the square of the modulus  $[(n_1^* - n_2^*) / (n_1^* + n_2^*)]$  [14] and has the form:

$$R = \frac{|n_1^* - n_2^*|^2}{|n_1^* + n_2^*|^2} = \frac{(n_1 - n_2)^2 + (k_1 - k_2)^2}{(n_1 + n_2)^2 + (k_1 + k_2)^2} \quad (2)$$

where  $n_1, n_2, k_1, k_2$  are the refractive indices and extinction coefficients of the material one and two, respectively. In case of glass substrate  $k=0$  and  $n$  values are calculated by Sellmeier dispersion equation and applied for quartz(SiO<sub>2</sub>) [15]:

$$n^2 = 1 + \frac{a_1 \lambda^2}{\lambda^2 - \lambda_1^2} + \frac{a_2 \lambda^2}{\lambda^2 - \lambda_2^2} + \frac{a_3 \lambda^2}{\lambda^2 - \lambda_3^2} \quad (3)$$

where  $a_1=0.6962$ ,  $a_2=0.4079$ ,  $a_3=0.8974$ ,  $\lambda_1=68$  nm,  $\lambda_2=116$  nm,  $\lambda_3=9896$  nm. The transmitted light that will

reach the absorber layer after reflection at all interfaces of solar cell is calculated by the following formula:

$$T_R(\lambda) = (1 - R_{12})(1 - R_{23})(1 - R_{34})(1 - R_{45}) \quad (4)$$

where  $R_{12}, R_{23}, R_{34}, R_{45}$  are the reflectivity of the interfaces air-glass, glass-TCO, TCO-CdS and CdS-PbS, respectively.

#### 2.1.2. Method two

In this method, the multiple reflection between any two layers will be considered. When the multi-reflections of  $L$  layers is taken into calculation (in the present case  $L=4$ ), the Eq. (4) can be expressed in the following form [16,17]:

$$T_R(\lambda) = 4 \frac{n_1 n_2}{(n_1 + n_2)^2} \prod_{j=2}^{L-1} \frac{4 \frac{n_j n_{j+1}}{(n_j + n_{j+1})^2}}{1 - \frac{(n_j - n_{j-1})^2 (n_j - n_{j+1})^2}{(n_j + n_{j-1})^2 (n_j + n_{j+1})^2}} \quad (5)$$

When the absorption in TCO and window layers is taken into account, the transmitted light reaching the absorber layer is given by [9]:

$$T(\lambda) = T_R(\lambda) (e^{-\alpha_1 d_1}) (e^{-\alpha_2 d_2}) \quad (6)$$

where  $\alpha_1, \alpha_2, d_1, d_2$  is the absorption coefficient and thickness of TCO material and CdS layers, respectively.

## 2.2. Recombination losses

Quantum efficiency of a solar cell always includes the drift and diffusion components, which are obliged to photogeneration of electron-hole pairs in the space charge region (SCR) and in the neutral part of the diode structure, respectively.

The drift component of the quantum efficiency includes the recombination at front surface of the absorber layer is given by [18]:

$$\eta_{drift} = \frac{1 + \frac{S}{D_p} \left( \alpha + \frac{2 \varphi_0 - qv}{W kT} \right)^{-1}}{1 + \frac{S}{D_p} \left( \frac{2 \varphi_0 - qv}{W kT} \right)^{-1}} \exp(-\alpha W) \quad (7)$$

where  $S$  is the front surface recombination velocity;  $v$  is the applied voltage;  $\varphi_0$  is the barrier height;  $D_p$  is the diffusion coefficient of holes related to their mobility  $\mu_p$  by the Einstein relation  $qD_p/kT = \mu_p$ ;  $W$  is the width of the space charge region;  $\alpha$  is the absorption coefficient of PbS at a given wavelength,  $q$  is the electron charge,  $k$  is the Boltzmann constant and  $T$  is room temperature.

The diffusion component of the quantum efficiency taking into account recombination at back surface of the

absorber layer is given by [19]:

$$\eta_{dif} = \frac{\alpha L_n}{\alpha^2 L_n^2 - 1} \exp(-\alpha W) \times \left[ \frac{S_b L_n}{D_n} \left[ \cosh\left(\frac{d-W}{L_n}\right) - \exp(-\alpha(d-W)) \right] + \sinh\left(\frac{d-W}{L_n}\right) + \alpha L_n \exp(-\alpha(d-W)) \right] \left( \alpha L_n - \frac{S_b L_n \sinh\left(\frac{d-W}{L_n}\right) + \cosh\left(\frac{d-W}{L_n}\right)}{D_n} \right) \quad (8)$$

where  $L_n = (\tau_n D_n)^{1/2}$  is the electron diffusion length;  $\tau_n$  is electron lifetime;  $D_n$  is the diffusion coefficient of electrons related to their mobility  $\mu_n$  by the Einstein relation  $qD_n/kT = \mu_n$ ,  $S_b$  is the velocity of recombination at the rear surface of the absorber layer and  $d$  its thickness.

The sum of equations (7) and (8) gives the expression of the internal quantum efficiency ( $\eta_{int}$ ).

$$\eta_{int} = \eta_{drift} + \eta_{dif} \quad (9)$$

It should be borne in mind that the recombination losses in space-charge region were not taken into current calculations.

When the reflectivity of metallic back contact is taken into consideration, the following formula [20] can be used to measure theoretically the effect of reflectivity from the back contact on the internal quantum efficiency:

$$\eta_{int}(R) = \eta_{int} [1 + R \exp(-\alpha d)] \quad (10)$$

where  $R$  is the reflectivity from the back contact,  $\alpha$  is the absorption coefficient of PbS layer and  $d$  its thickness.

### 2.3. Short-circuit current density

If  $\Phi_i$  is the spectral radiation power density and  $h\nu$  is the photon energy, the spectral density of the incident photon flux is  $\Phi_i/h\nu$ , and then the short-circuit current density  $J_{SC}$  is given by [9, 18]:

$$J_{SC} = q \sum_i T(\lambda) \frac{\phi_i(\lambda_i)}{h\nu_i} \eta(\lambda_i) \Delta\lambda_i \quad (11)$$

where  $T(\lambda)$  is the optical transmission and  $\Delta\lambda_i$  is the interval between the two neighboring values  $\lambda_i$ . The calculations will be done for AM1.5 solar radiation using Tables ISO 9845-1:1992 (Standard ISO, 1992) [21].

### 2.4. Cell parameters of CdS/PbS heterojunction

The  $J-V$  characteristic under illumination of CdS/CdTe solar cells can be presented as:

$$J(V) = J_d - J_{ph} \quad (12)$$

where  $J_{ph}$  is the photocurrent density. In this work, the dark current  $J_d(V)$  of efficient thin-film CdS/CdTe cells is quantitatively described in terms of the Sah–Noyce–Shockley theory of generation–recombination in the space–charge region of the heterostructure [22]. More details of calculation  $J_d(V)$  can be found elsewhere [23–25].

### 3. Results and discussion

Fig. 1 shows the calculation of spectral reflection coefficient  $R(\lambda)$  at interface TCO-air (Fig. 1-a) and TCO-glass (Fig. 1-b) for different TCO materials (ZnO, ZnO:SnO<sub>2</sub>, ZnO:Al and ZnO:In) that are used as front electrode in CdS/PbS solar cells. The results in Fig.1 are carried out based on Eq. 2, which is dependent on the refractive index ( $n$ ) and extinction coefficient ( $k$ ) of TCOs, air and glass. The data of  $n$  and  $k$  of ZnO, ZnO:Sn, ZnO:Al, and ZnO:In, are taken from Refs. [26], [27], [28] and [29], respectively. The extinction coefficient ( $k$ ) value of glass substrate was taken as  $k=0$ . while, the Sellmeier dispersion equation (Eq. 3) has been applied for calculating the refractive index of glass substrate [15]. It is clear that the given values of reflection coefficient are in the range 0.07–0.18 in the case of TCO-glass. While low values of  $R(\lambda)$  (in the range 0.008 – 0.06) are obtained in the case of TCO-air due to the small difference between the optical constants of TCO material and glass. Besides, ZnO:Al and ZnO:In represent the minimum value of  $R(\lambda)$  compared with the other TCO electrodes. The result indicates a small part of the incident photons will be lost before reaching the absorber layer due to reflection at TCO-glass interface.

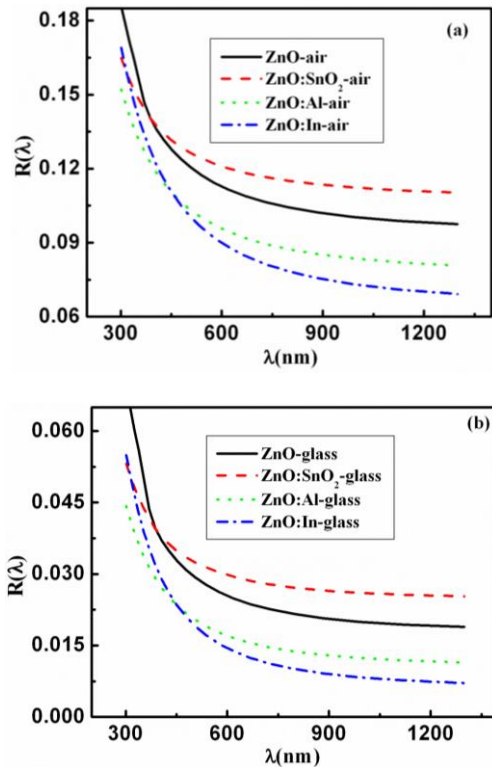


Fig. 1. Calculated reflection spectra ( $R$ ) of different TCO material (ZnO, ZnO:Sn, ZnO:Al, ZnO:In) that used as front electrode in CdS/PbS solar cells in the case of a) air and b) glass

Equations 4 and 5 give the transmission coefficient  $T(\lambda)$  due to the reflection (method 1, Eq.4) as well as the transmission coefficient due to multiple reflections (method 2, Eq.5) at all interfaces air-glass, glass-TCO, TCO-CdS and CdS-PbS. The average of  $T(\lambda)$  in the wavelength range of 450-1200 nm is calculated and plotted in Fig. 2-1 for various TCO material, which are used as a front electrode in CdS/PbS solar cells. It is clear that the multiple reflection effect (method 2) is more significant comparing with method 1. Where the average transmission is about 88.5 % according to method (2) and about 86.5 % according to method 1. Moreover, when ZnO:Al is used as a front electrode, the transmission reaches its maximum value in both methods. The spectral transmission coefficient  $T(\lambda)$  at CdS/PbS interface is calculated using Eq.6 for different TCO materials and plotted in Fig.2-b. This figure includes the effect of absorption process that takes place in TCO and CdS layers on the transmission spectra. These results are carried out using method (2) (multiple reflections) and at 100 nm thickness of both TCO and CdS layers. Comparing the current results with the results from Fig.(2-a), a small decrease in  $T(\lambda)$  at  $\lambda > 550$  nm can be observed and much more decrease in transmission can be seen at  $\lambda > 500$  nm due to a significant effect of absorption process in high absorption region. The inset figure shows the average transmission in the wavelength range of 450-1200 nm. As can be seen, the maximum average transmission of 69% is achieved for ZnO:Al. Comparing this result with the result

of Fig. (2-a), it can be concluded that the reflection loss is about 12% and the optical losses (reflection and absorption) are about 32%, which indicates that the absorption process in both ZnO:Al and CdS layers leading to a decrease in the transmitted light that reaches the absorber layer by a ratio of 21%. Much more optical losses can be observed for the others TCO materials. Besides, decreasing the thickness of TCO and CdS layer will produce a great effect in transmission spectra. It is known, however, that it is difficult to obtain uniform and pin-hole free CdS layers thinner than 50 nm[30]. More accurate value of optical losses will be obtained when the short-current density is calculated.

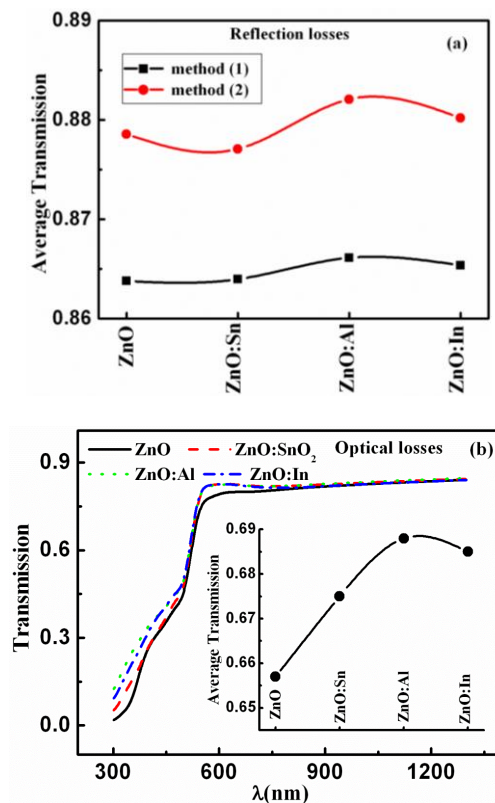


Fig. 2. Calculated transmission spectra of different TCO material (ZnO, ZnO:Sn, ZnO:Al, ZnO:In) that used as front electrode in CdS/PbS solar cells due to a) reflection (method 1) and multiple reflections (method 2) at different interfaces and b) multiple reflection at different interfaces and absorption in TCO and CdS layers. The inset is the average transmission in the wavelength range of 400-1300 nm

In order to estimate the level of recombination losses for CdS/PbS solar cells, the internal quantum efficiency ( $\eta_{int}$ ) must be calculated at various parameters. According to Eqs.7-10, the internal quantum efficiency depends on some parameters such as; the absorption coefficient of PbS, the width of space-charge region, the thickness of PbS, the electron diffusion length, the front and back surface recombination velocity and the barrier height. The variation of absorption coefficient with wavelength of PbS layer is calculated from  $(4\pi k/\lambda)$ . Moreover, the values of

other parameters (except the thickness of PbS and the width of space-charge region) is listed in Table 1. In this section, the dependence of  $\eta_{\text{int}}$  on the width of space-

charge region ( $W$ ) and on the thickness of PbS layer ( $d_{\text{PbS}}$ ) will be discussed in detail.

Table 1. The values of the parameters that are used in this study

Parameter	Value	Ref.
Thickness of TCO, $d_1$	100 nm	[10]
Thickness of CdS, $d_2$	100 nm	[10]
$\Phi_0$ -qV	1 eV	Current work
Hole diffusion coefficient, $\mu_p$	80 $\text{cm}^2/(\text{V S})$	[10]
Electrons related mobility, $\mu_n$	1000 $\text{cm}^2/(\text{V S})$	[10]
Front surface recombination velocity, $S$	$10^7$ cm/sec	[8]
Back surface recombination velocity, $S_b$	$10^7$ cm/sec	[8]
electron lifetime, $\tau_n$	$10^{-8}$ s	Current work

The dependence of spectral quantum efficiency ( $\eta_{\text{int}}$ ) on the width of space-charge region ( $W$ ) at  $d_{\text{PbS}}=3 \mu\text{m}$  is shown in Fig.3-a. The results presented in Fig. 3-a show that  $\eta_{\text{int}}$  increases with increasing the energy of incident photons. Besides, an increase in  $\eta_{\text{int}}$  can be observed with increasing the width of space-charge region ( $W$ ). This behaviour is not expected because the increasing of  $W$  leads to decrease the strength of electric field inside the space-charge region and hence the probability of separation of the generated photo-carriers is decreasing. This behaviour can be attributed to a great portion of incident photons is absorbed outside the space-charge region (i.e. in the neutral part of PbS) [7, 8] because of the absorption coefficient of PbS is small comparing with CdTe absorber. According to Eq. 9, the internal quantum efficiency is the sum of two components; the drift component ( $\eta_{\text{drift}}$ ) which is given by Eq. 7 and it takes into account the recombination losses at front surface of PbS and the diffusion component ( $\eta_{\text{dif}}$ ) which is given by Eq.8 and it takes into account the back surface recombination losses. The spectral distribution of  $\eta_{\text{drift}}$  at various widths of  $W$  is plotted in Fig3-b. It is clear that  $\eta_{\text{drift}}$  has the same behaviour of  $\eta_{\text{int}}$ . In general the value of  $\eta_{\text{int}}$  is smaller than unity particularly at high wavelength indicating a significant role of front surface recombination losses. On the other hand, the dependence of spectral  $\eta_{\text{dif}}$  on  $W$  is shown in Fig.3-c. As can be seen, the diffusion component of internal quantum efficiency is decreasing with increasing the width of space-charge region due to the decrease of the value of  $(d-W)$  that appears in Eq.8 and thus decreasing the thickness of neutral part of the absorber layer. It is clear that the contribution of  $\eta_{\text{dif}}$  in collecting the photo-generated carriers is smaller than the contribution of  $\eta_{\text{drift}}$ .

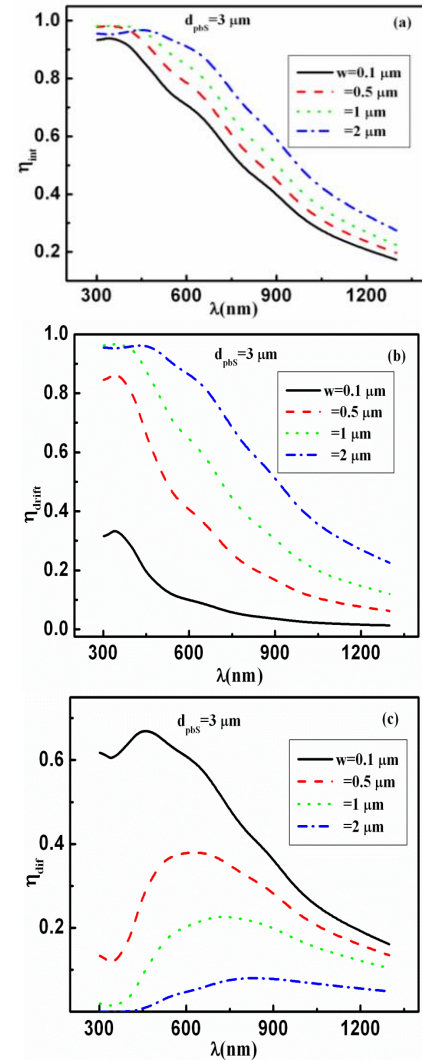


Fig. 3. a) Internal quantum efficiency ( $\eta_{\text{int}}$ ) spectrum, b) drift component of internal quantum efficiency ( $\eta_{\text{drift}}$ ) spectrum and c) diffusion component of internal quantum efficiency ( $\eta_{\text{dif}}$ ) spectrum at  $3 \mu\text{m}$  thickness of PbS ( $d_{\text{PbS}}$ ) and at different values of the width of space-charge region ( $w$ )

Fig. 4-a shows the effect of thickness of PbS layer on the spectral quantum efficiency at width of space-charge region of  $1 \mu\text{m}$ . It is clear that the behaviour of  $\eta_{\text{int}}$  in this figure is the same of its behaviour in Fig. 3-a. It can be seen that with increasing the thickness of absorber layer from  $1.5$  to  $3 \mu\text{m}$  the value of  $\eta_{\text{int}}$  increases. This behaviour can be explained in terms of diffusion component of internal quantum efficiency. From Eqs. 7&8, it can be observed that the diffusion component only depends on the thickness of the absorber layer. Therefore, Fig. 4-b shows the dependence of diffusion component of internal quantum efficiency ( $\eta_{\text{dif}}$ ) on the thickness of PbS layer. The increase of  $\eta_{\text{dif}}$  is attributed to the increase of the thickness of the neutral part of PbS and then increase the probability to absorb the incident photons outside the space-charge region. Comparing the values of  $\eta_{\text{int}}$  and  $\eta_{\text{dif}}$ , it can be concluded that the contribution of diffusion component can be ignored particularly at small thickness of the absorber layer and the main value of  $\eta_{\text{int}}$  is due to the drift component of internal quantum efficiency even at larg thickness ( $3 \mu\text{m}$ ) of the absorber layer.

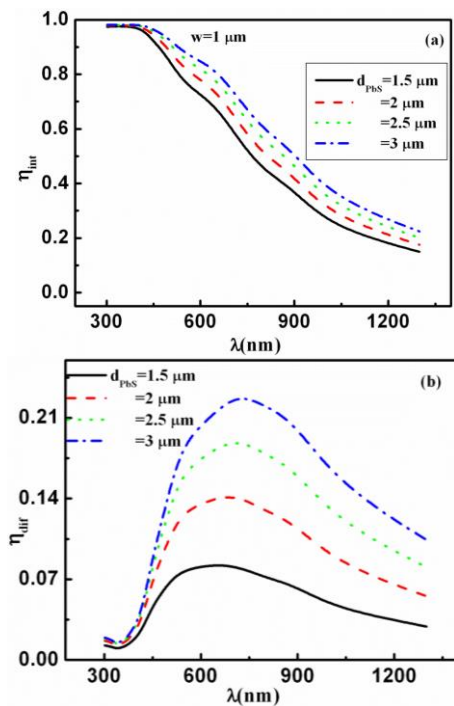


Fig. 4. a) Internal quantum efficiency ( $\eta_{\text{int}}$ ) spectrum at space-charge region width ( $w$ ) of  $1 \mu\text{m}$  and b) diffusion component of internal quantum efficiency ( $\eta_{\text{dif}}$ ) spectrum at different thicknesses of PbS layer ( $d_{\text{PbS}}$ )

The variation of short-circuit current density ( $J_{\text{SC}}$ ) with the width of space charge region and with the thickness of absorber layer for various transparent electrodes is shown in Fig. 5. Fig. 5-a shows the dependence of  $J_{\text{SC}}$  on  $W$  at  $d_{\text{PbS}} = 3 \mu\text{m}$  for various materials that are used as a front electrode in CdS-PbS

cells. It can be seen that  $J_{\text{SC}}$  increases with increasing the width of space-charge region and records values of  $14.7\text{--}20 \text{ mA/cm}^2$  for ZnO layer. Moreover,  $J_{\text{SC}}$  represents the maximum values of  $15.4\text{--}20.9 \text{ mA/cm}^2$  in the case of ZnO:Al. When  $T=1$ ,  $\eta=1$  in Eq.11,  $J_{\text{SC}}$  records a value of  $\sim 41 \text{ mA/cm}^2$ . Besides, the maximum optical and recombination losses of about 64% are observed in the case of ZnO at  $0.1$  width of the space-charge region. While, the minimum losses of about 62% are observed when ZnO:Al is used as a front electrode. With increasing the width of the space-charge region, the losses are decreased and record a value of 51% at  $W=2 \mu\text{m}$  for ZnO:Al electrode. The decrease of these losses is resulted in the decrease of recombination losses with increasing the width of space-charge region (see the increase of  $\eta_{\text{int}}$  with  $W$  as shown in Fig. 3-a).

The dependence of  $J_{\text{SC}}$  on the thickness of PbS at  $W=1 \mu\text{m}$  is shown in Fig.5-b. It can be seen that at  $d_{\text{PbS}}=1.5 \mu\text{m}$ ,  $J_{\text{SC}}$  exhibits its low value of  $14.4 \text{ mA/cm}^2$  for ZnO and its maximum value of  $18.9 \text{ mA/cm}^2$  for ZnO:Al. With increasing the thickness of PbS from  $1.5 \mu\text{m}$  to  $3 \mu\text{m}$ , the above values of  $J_{\text{SC}}$  increased and record  $18 \text{ mA/cm}^2$  and  $18.9 \text{ mA/cm}^2$  for ZnO and ZnO:Al, respectively. According to these results and at  $d_{\text{PbS}}=1.5 \mu\text{m}$ , the maximum optical and recombination losses are about 64.7% and 56% for ZnO and ZnO:Al, respectively. The minimum optical and recombination losses are about 62% and 54% for ZnO and ZnO:Al, respectively. Comparing the results from Fig. 5-a and Fig. 5-b, it can be concluded that the influence of width of space-charge region is slightly more effective than the influence of the thickness of absorber layer.

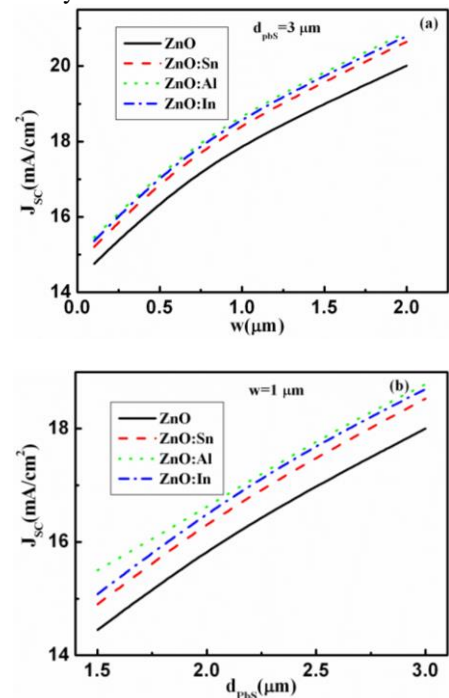


Fig. 5. Short-circuit current density ( $J_{\text{SC}}$ ) of CdS/PbS calculated at various TCO materials (ZnO, ZnO:Sn, ZnO:Al, ZnO:In) that used as front electrode as a function of a) width of space-charge region ( $w$ ) at  $d_{\text{PbS}} = 3 \mu\text{m}$  and b) PbS thickness ( $d_{\text{PbS}}$ ) at  $w = 3 \mu\text{m}$

It is reported in Ref. 22, the reflectivity from back contact has a significant effect on the internal quantum efficiency and hence on the value of short-circuit current density particularly at thin thickness of the absorber layer. In our current case, the thickness of PbS is varied from 1.5  $\mu\text{m}$  to 3  $\mu\text{m}$  then the effect of reflectivity from back contact must be taken into consideration. Fig. 6 shows the short-circuit current density ( $J_{SC}$ ) of CdS/PbS calculated at various TCO materials (ZnO, ZnO:Sn, ZnO:Al, ZnO:In) that used as front electrode as a function of different ratios of reflectivity from back contact (R%) at  $w=1\ \mu\text{m}$  and  $d_{PbS}=3\ \mu\text{m}$ . It is clear that with increasing the reflectivity from back contact from R=0% to R=100% (PbS is completely reflected), the value of  $J_{SC}$  increases and attains its maximum value of 22.3  $\text{mA}/\text{cm}^2$  for ZnO:Al. To estimate the contribution of reflectivity from back contact on the increasing of  $J_{SC}$  values, Fig. 6-b shows the ratio of increasing  $J_{SC}$  with increasing the ratio of reflectivity. It is clear that the reflectivity from metallic back contact leads to increase the short-circuit current density by a ratio reaches  $\sim 20\%$  when the back contact is totally reflected (R=100%).

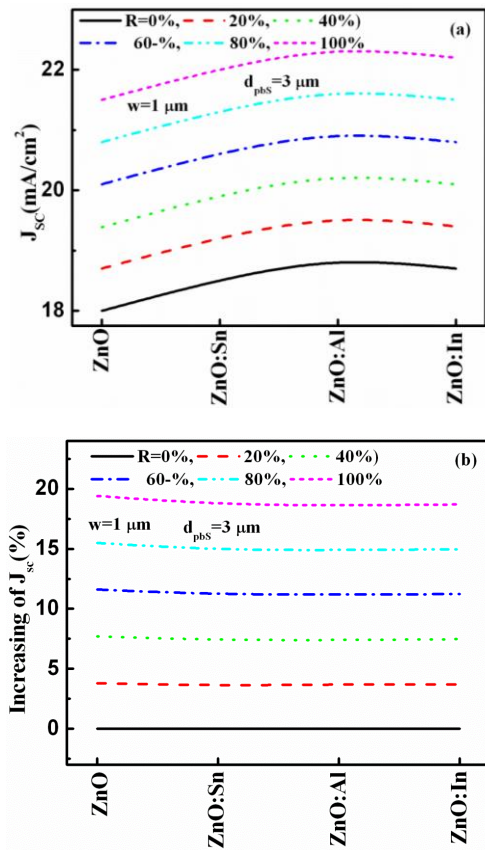


Fig. 6. Short-circuit current density ( $J_{SC}$ ) of CdS/PbS calculated at various TCO materials (ZnO, ZnO:Sn, ZnO:Al, ZnO:In) that used as front electrode a) as a function of different ratios of reflectivity from back contact (R%) at  $w=1\ \mu\text{m}$  and  $d_{PbS}=3\ \mu\text{m}$  and b) the corresponding increasing ratio of  $J_{SC}$

Fig. 7 shows the  $J$ - $V$  characteristic curves of CdS/PbS solar cells at various TCO materials (ZnO, ZnO:Sn, ZnO:Al, ZnO:In) that used as front electrode at different values of reflectivity from back contact. The results shown in this figure are carried out under illumination condition of AM1.5 solar irradiation (ISO 9845-1:1992) [21]. It is clear that with increasing the reflectivity from back contact from R=0% to R=100% the  $J$ - $V$  curves are shifted down and the maximum shift is observed for ZnO:Al electrode. From this figure some important cell parameters such as fill factor (FF), open circuit voltage ( $V_o$ ), output power density ( $P_{out}$ ) and cell efficiency ( $\eta$ ) can be estimated.

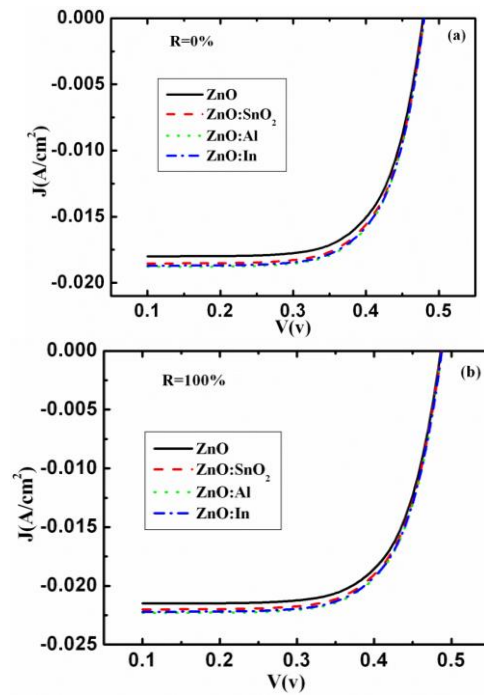


Fig. 7.  $J$ - $V$  curves of CdS/PbS solar cells at various TCO materials (ZnO, ZnO:Sn, ZnO:Al, ZnO:In) that used as front electrode at reflectivity from back contact of a) R=0% and b) R=100%.

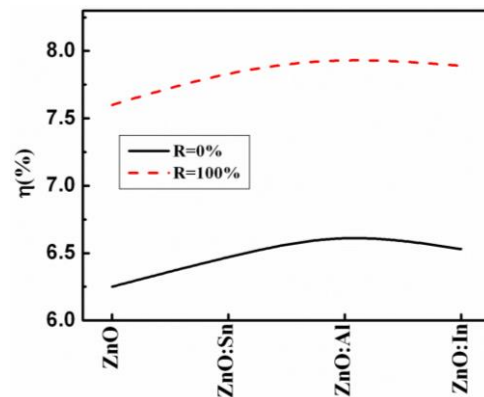


Fig. 8. Efficiency ( $\eta$ ) of CdS/PbS solar cells at various TCO materials (ZnO, ZnO:Sn, ZnO:Al, ZnO:In) that used as front electrode at reflectivity from back contact of R=0% and 100%

The efficiency of CdS-PbS cell is shown in Fig. 8 for various TCO materials (ZnO, ZnO:Sn, ZnO:Al, ZnO:In) that are used as front electrode at different values of reflectivity from back contact. A maximum efficiency of 6.61% is achieved for ZnO:Al and this ratio increased up to 7.89% with increasing ratio of 20% at 100% reflectivity from back contact. The other cell parameters such as FF,  $V_o$  and  $P_{out}$  are computed and listed in Table 2. It is clear

that the fill factor is approximately fixed at 70% for difference TOC materials. The maximum open circuit voltage of 479 mV is observed for ZnO:Al and this value increased up to 487 mV at 100% reflectivity from back contact and the corresponding values of  $P_{out}$  are 6.37 mW/cm<sup>2</sup> and 7.64 mW/cm<sup>2</sup> for R=0% and R=100%, respectively.

Table 2. The fill factor (FF), output power density ( $P_{out}$ ), and open circuit voltage ( $V_o$ ) of CdS/PbS solar cell at transparent conductive oxides (TCOs), which were used as front electrode at zero and 100% reflectivity (R %) from metallic back contact

TCOs	FF(%)		$P_{out}$ (mW/cm <sup>2</sup> )		$V_o$ (v)	
	R=0%	R=100%	R=0%	R=100%	R=0%	R=100%
ZnO	70.37	70.19	6.05	7.30	0.478	0.485
ZnO:Sn	70.63	70.60	6.25	7.55	0.478	0.486
ZnO:Al	70.80	70.34	6.37	7.64	0.479	0.487
ZnO:In	70.33	70.46	6.28	7.60	0.479	0.486

#### 4. Conclusions

Thin film photovoltaic solar cells CdS/PbS require the use of transparent conductive materials (TCOs) as a front electrodes electrode. These electrodes must be abundant, inexpensive and enable efficient thin film solar cells. This work investigated the using of low cost ZnO, ZnO:Sn, ZnO:Al and ZnO:In as a front electrode in CdS-PbS thin film solar cells. Two methods were employed to calculate the transmitted light that will reach the absorber layer. The first method was carried out based on the reflection at difference interfaces; air-glass, glass-TCO, TCO-CdS and CdS-PbS. While the second method was based on the multiple reflections effect at these interfaces. It was found that the second method was more significant comparing with first method. Where the average transmission was about 88.5 % according to second method and about 86.5 % according to first method. With computing the transmission and internal quantum efficiency, the optical and recombination losses were estimated. The maximum optical and recombination losses of about 64% were observed in the case of ZnO at 0.1  $\mu$ m width of the space-charge region and 3  $\mu$ m thickness of the absorber layer. While, the minimum losses of about 62% were observed when ZnO:Al was used as a front electrode under the above conditions. The reflectivity form metallic back contact led to increase the short-circuit current density and the cell efficiency by a ratio reached ~ 20% when the back contact was totally reflected. The maximum output power density of 7.64 mW/cm<sup>2</sup>, maximum open circuit voltage of 487 mV and the maximum cell efficiency of 7.9% were achieved for ZnO:Al electrode at 100% reflectivity from back contact.

#### Acknowledgment

This project was supported by King Saud University, Deanship of Scientific Research, College of Sciences Research Center.

#### References

- [1] J. H. Borja, Y. V. Vorobiev, R. R. Bon, Sol. Energy Mater. Sol. Cells **95**, 1882 (2011).
- [2] N.R. Mathews, C. A.Chavez, M. A. C. Jacome, J. A. T. Antonio, Electrochimica. Acta **99**, 76 (2013).
- [3] H. Moreno-Garcia, M. T. S. Nair, P. K. Nair, Thin Solid Films **519**, 2287 (2011).
- [4] A. S. Obaid, M. A. Mahdi, Z. Hassan, M. Bououdina, Superlattice. Microst. **52**, 816 (2012).
- [5] A. S. Obaid, M. A. Mahdi, Z. Hassan, M. Bououdina, Int. J. hydrogen energy. **38**, 807 (2013).
- [6] R. J. Ellingson, M. C. Beard, J. C. Johnson, P. Yu, O. I. Micic, A. J. Nozik, A. Shabaev, A. L. Efros, Nano Letters **5**, 865 (2005).
- [7] H. A. Mohamed, Solar energy **108**, 360 (2014).
- [8] H. A. Mohamed, Philosophical Magazine **94**, 3467 (2014).
- [9] H. A. Mohamed, J. Appl. Phys. **113**, 093105 (2013).
- [10] A. M. Acevedo, Sol. Energy **80**, 675 (2006)
- [11] S. H. Jeong, S. B. Lee, J.-H. Boo, Curr. Appl. Phys. **4**, 655 (2004).
- [12] A. Goyal, S. Kachhwaha, Mater. Lett. **68**, 354 (2012).
- [13] K. Kim, S. Kimb, S. Y. Lee, Curr. Appl. Phys. **12**, 585 (2012).
- [14] T. S. Moss, G. J. Burrel, D. Ellis, Semiconductor Opto-Electronics, Butterworth Publishers, New York, 1973, pp. 12–17.
- [15] S. O. Kasap, Optoelectronics and Photonics: Principles and Practice, Prentice Hall, New Jersey, 2000, p. 45.
- [16] F. W. Mont, J. K. Kim, M. F. Schubert, H. Luo, E. F. Schubert, R. W. Siegel, Proc. SPIE **6486**, 64861C (2007).
- [17] F. W. Mont, J. K. Kim, M. F. Schubert, E. F. Schubert, R. W. Siegel, J. Appl. Phys. **103**, 083120 (2008).
- [18] L. A. Kosyachenko, A. I. Savchuk, E. V. Grushko, Thin Solid Films **517**, 2386 (2009).

- [19] V. V. Brus, *Solar Energy* **86**, 786 (2012).
- [20] N. R. Paudel, K. A. Wieland, A. D. Compaan, *Sol. Energy Mater. Sol. Cells* **105**, 109 (2012).
- [21] Reference Solar Spectral Irradiance at the Ground at Different Receiving Conditions, Standard of International Organization for Standardization ISO 9845-1, 1992
- [22] H. A. Mohamed, *thin solid films* **589**, 72 (2015).
- [23] C. Sah, R. Noyce and W. Shockley, *Proceedings of the IRE* **46**, 1228 (1957).
- [24] S. M. Sze, *Physics of Semiconductor Devices*, 2nd ed. Wiley, New York, (1981).
- [25] L. A. Kosyachenko, O. L. Maslyanchuk, V. V. Motushchuk, V. M. Sklyarchuk, *Sol. Energy Mater. Sol. Cells* **82**, 65 (2004).
- [26] S.W. Xue, X.T. Zu, W.L. Zhou, H.X. Deng, X. Xiang, L. Zhang, H. Deng, *J. Alloy. Compd.* **448**, 21 (2008).
- [27] E. Çetinörgü, *Opt. Commun.* **280**, 114 (2007).
- [28] Q. Xu, R. D Hong, H. L Huang, Z. F Zhang, M. K. Zhang, X.P Chen, Z. Y. Wu, *Opt. Laser Technol.* **45**, 513 (2013).
- [29] G. C. Xie, L. Fang, L. P. Peng, G. B. Liu, H. B. Ruan, F. Wu, C. Y. Kong, *Phys. Procedia* **32**, 651 (2012 )
- [30] L. A. Kosyachenko, E. V. Grushko, X. Mathew, *Sol. Energy Mater. Sol. Cells* **96**, 231 (2012).

---

\*Corresponding author: hussein\_abdelhafez2000@yahoo.com